Available online at www.sciencedirect.com
ScienceDirect
Catalysis Today 126 (2007) 351–358
CATALYSIS TODAY
www.elsevier.com/locate/cattod

Copper-impregnated Al–Ce-pillared clay for selective catalytic reduction of NO by C_3H_6

Qichun Lin [a], Jiming Hao [a,*], Junhua Li [a], Zifeng Ma [b], Weiming Lin [c]

[a] Department of Environmental Science and Engineering, Tsinghua University, Beijing 100084, PR China
[b] Department of Chemical Engineering, Shanghai Jiao Tong University, Shanghai 200240, PR China
[c] Department of Chemical Engineering, Guangzhou University, Guangzhou 510405, PR China

Available online 17 July 2007

Abstract

The selective catalytic reduction (SCR) of NO by hydrocarbon is an efficient way to remove NO emission from lean-burn gasoline and diesel exhaust. In this paper, a thermally and hydrothermally stable Al–Ce-pillared clay (Al–Ce-PILC) was synthesized and then modified by SO_4^{2-}, whose surface area and average pore diameter calcined at 773 K were 161 m^2/g and 12.15 nm, respectively. Copper-impregnated Al–Ce-pillared clay catalyst (Cu/SO_4^{2-}/Al–Ce-PILC) was applied for the SCR of NO by C_3H_6 in the presence of oxygen. The catalyst 2 wt% Cu/SO_4^{2-}/Al–Ce-PILC showed good performance over a broad range of temperature, its maximum conversion of NO was 56% at 623 K and remained as high as 22% at 973 K. Furthermore, the presence of 10% water slightly decreased its activity, and this effect was reversible following the removal of water from the feed. Py-IR results showed SO_4^{2-} modification greatly enhanced the number and strength of Brönsted acidity on the surface of Cu/SO_4^{2-}/Al–Ce-PILC, which played a vital role in the improvement of NO conversion. TPR and XPS results indicated that both Cu^+ and isolated Cu^{2+} species existed on the optimal catalyst, mainly Cu^+, as Cu content increased to 5 wt%, another species CuO aggregates which facilitated the combustion of C_3H_6 were formed.

Keywords: Cu/SO_4^{2-}/Al–Ce-PILC; SCR of NO; C_3H_6; Acidity; Copper species

1. Introduction

Nitric oxides (NO_x) from combustion facilities are the main pollutants that contribute to the formation of acid-rain, smog, and ground level ozone. Therefore, stringent regulations around the world [1–3] have led to the development of efficient DeNO_x technologies. To date, much research related to the SCR of NO by hydrocarbons (HCs) has been undertaken and reported in the literature due to its potential application for lean-burn gasoline and diesel engines, where the noble-metal three-way catalysts do not work well in the presence of excess oxygen [4]. Many classes of catalysts, including supported noble metals (e.g. Pt, Pd, Rh, and Au) [5–10], metal oxides (e.g. CuO, Ag_2O, SnO_2, and In_2O_3) [5,11–18], and zeolite types (e.g. Cu-ZSM-5, Cu-Al-MCM-41) [19–23], have been investigated in the HC-SCR reaction. Among them, metal-exchanged ZSM-5 has been widely examined due to higher NO removal than for other catalysts. However, the catalyst was low thermal stability and severe deactivation by H_2O. Hence, continuing efforts are made to develop new catalysts.

Pillared interlayered clays (PILCs) offer good possibilities. They are two-dimensional zeolite-like materials prepared by exchanging charge-compensating cations between clay layers with large inorganic metal hydroxycations, which are oligomeric and are formed by hydrolysis of metal oxides or salts [24]. After heating, the intercalated species undergo dehydration and dehydroxylation to form stable metal oxide clusters that act as pillars keeping the silicate layers apart and creating interlayer spaces. Since PILCs have a number of attractive features, such as a well-developed two-dimensional structure, tunable pore size, high thermal stability, and exchangeable acidity, they have attracted much attention as potential catalyst materials in many reaction systems, including SCR reactions [4,25–27]. It has been reported that metal-exchanged PILCs were more tolerant to H_2O and SO_2 than metal-exchanged zeolites [4].

In the present study, montmorillonite was pillared by multi-oligomeric hydroxyl cations to synthesize Al–Ce-PILC, and

* Corresponding author. Tel.: +86 10 62782195; fax: +86 10 62773650.
E-mail address: hjm-den@mail.tsinghua.edu.cn (J. Hao).

0920-5861/$ – see front matter © 2007 Elsevier B.V. All rights reserved.
doi:10.1016/j.cattod.2007.06.007

then modified by SO_4^{2-}. Cu/SO_4^{2-}/Al–Ce-PILC catalysts were prepared by impregnation and applied to the reduction of NO by C_3H_6 in excess oxygen. The influence of SO_4^{2-} modification and Cu content on the catalytic performance was investigated. The physical properties of Al–Ce-PILC were evaluated by powder XRD and BET, and Cu/SO_4^{2-}/Al–Ce-PILC was characterized by Py-IR, TPR, and XPS in order to relate the chemical properties of the catalysts to their performance. Finally, the effect of water vapor on the catalytic performance and the structure of the catalyst were studied.

2. Experimental

2.1. Synthesis of Al–Ce-PILC

The starting clay used in this study was a purified sodium-exchanged Xinyang montmorillonite, which had a particle size of 2 μm or less and a cation-exchange capacity (CEC) of 80 meq./100 g.

Pillared clays incorporated with alumina and rare earth were synthesized according to the procedure described in Ref. [28]. A suitable volume of 0.2 mol/dm^3 NaOH was added dropwise to a stirred solution of 0.2 mol/dm^3 $AlCl_3$ + $CeCl_3$ in order to obtain an OH/(Al + Ce) mole ratio of 2.0. The Al/Ce mole ratio was kept at 5. The resulting solution was aged for 7 days at room temperature and then heated at 333 K for 2 h before the pillaring process. In a typical pillaring procedure, the Na-montmorillonite (Na-Mont) was dispersed in deionized water to form a 1.0 wt% clay slurry. The slurry was then stirred at room temperature for 24 h to improve its dispersion. The amount of Al–Ce pillaring solution required to obtain an (Al + Ce)/Na-Mont content of 10 mmol/g was then added dropwise to the clay slurry. The mixture was stirred for 3 h at 333 K, and then washed with deionized water until free of chloride ($AgNO_3$ test). The sample was then dried in air at 333 K for 24 h and calcined at 773 K for 6 h. Subsequently, Al–Ce-PILC was impregnated in a suitable volume of 0.5 mol/dm^3 $(NH_4)_2SO_4$ at 333 K for 1 h with stirring. After filtration, the sample was first dried at 383 K in air for 12 h and then calcined at 773 K for another 6 h to obtain Al–Ce-PILC with SO_4^{2-} modification (SO_4^{2-}/Al–Ce-PILC).

2.2. Catalyst preparation

Cu-based catalysts were prepared by impregnating Al–Ce-PILC or SO_4^{2-}/Al–Ce-PILC with a cupric nitrate solution. The copper content of the catalysts was adjusted by changing the concentration of the aqueous $Cu(NO_3)_2$ solution (the minimum volume required to wet the solid). After impregnation for 6 h, the solvent was evaporated under an infrared lamp. The samples were then dried and calcined at 773 K for 6 h.

2.3. Characterization

X-ray powder diffraction (XRD) patterns were measured with a Shimadzu Model XD-610 diffractometer, and Ni-filtered Cu Kα radiation (λ = 1.5415 Å) was utilized in an X-ray tube operated at 30 kV and 200 mA.

N_2 adsorption was determined at 77 K on a TriStar 3000 Micromeritics instrument. The samples were previously degassed at 523 K for 2 h. Specific surface areas were calculated by the BET method. For porosity analysis, the BJH method was used.

The FT-IR spectra of chemisorbed pyridine (Py-IR) were obtained on a Perkin-Elmer Model 2000 spectrophotometer in the 1750–1420 cm^{-1} range. The self-supported sample wafers were outgassed at 773 K for 1 h prior to pyridine adsorption. After the adsorption of pyridine at room temperature, the catalysts were outgassed at 373, 473, 573, and 673 K, and their spectra were recorded.

Temperature programmed reduction (TPR) measurements were made to identify the copper species and their reducibility on the catalyst surface. 0.05 g sample of catalyst was charged in a U-shape quartz microreactor. It was then outgassed by heating at 15 K/min in a helium flow (20 ml/min) up to 773 K, kept at this temperature for 30 min, then was cooled to room temperature and stabilized under an Ar/H_2 flow (99.9990% purity, 95/5 volumetric ratio, 20 ml/min). The temperature and detector signals were continuously recorded with heating of 10 K/min up to 973 K.

To identify the state of the copper on the catalyst surface, X-ray photoelectron spectroscopy (XPS) was examined by a Physical Electronics Company Quantum-2000 Scanning ESCA Microprobe that used an Al Kα radiation source. The charging effect of the XPS spectra was calibrated by justifying the carbon (1 s) line at 284.6 eV associated with hydrocarbon impurities on the catalyst surface.

2.4. Catalytic activity measurement

Catalytic activity was measured in a fixed-bed quartz flow reactor at a flow rate of 200 ml/min and a space velocity (GHSV) of 24,000 h^{-1}. The reaction temperature was controlled by a programmable temperature controller. The catalyst was preconditioned at each reaction temperature for 30 min before the analysis was started. The feed composition was 1200 ppm C_3H_6, 2200 ppm NO, 2% O_2, and 10% H_2O (when used), and helium was used as balance. Water vapor was generated by passing helium gas through a gas-wash bottle containing deionized water. The reactants and products were analyzed by on-line gas chromatography (Shimadzu GC 17A) and a chemiluminescence NO/NO_2/NO_x analyzer (Thermo Environmental Instruments, model 42C). The GC columns used were Porapak Q for separation of N_2O, CO_2, and C_3H_6, and molecular sieve 5 Å for separating of O_2, N_2, and CO. The N_2O concentration leaving the reactor was below a conservative estimate of the limit of detection (<10 ppm) and so will not be further discussed. The catalytic activity was evaluated in terms of NO and C_3H_6 conversion defined as follows:

$$X_{NO} = \frac{[N_2]}{2[NO]_0} \times 100\%,$$

$$X_{C_3H_6} = \frac{[C_3H_6]_0 - [C_3H_6]}{[C_3H_6]_0} \times 100\%.$$

3. Results and discussion

3.1. XRD

Fig. 1a and b shows the XRD patterns of the parent Na-Mont and the Al–Ce-PILC calcined at different temperatures, respectively. The parent Na-Mont showed a relatively broad and intense reflection at $2\theta = 6.9^{\circ}$, with basal spacing of 12.7 Å, which was commonly assigned to the basal (0 0 1) reflection. The basal spacing, $d_{0\,0\,1}$, represented the distance between two clay layers, including the thickness of one of the layers. This peak was shifted to lower 2θ values for all the Al–Ce-PILC samples, which was a clear indication of the enlargement of the basal spacing of the clay as a result of pillaring. The $d_{0\,0\,1}$ basal spacing of the uncalcined Al–Ce-PILC was 20.5 Å, which was much larger than that of Na-Mont. Upon calcination at 773 K, the $d_{0\,0\,1}$ peak of Na-Mont nearly disappeared, which reflected serious damage and loss of crystallinity in the clay layer, since the weak electrostatic and other forces operating between the clay layers cannot retain the layer structure of the clay materials at high temperatures. However, the $d_{0\,0\,1}$ peaks of Al–Ce-PILCs shifted to a lightly higher 2θ values, indicating a slight reduction in the interlayer spacing. When the sample was calcined at 973 K, the $d_{0\,0\,1}$ peak also shifted to higher angles and widened, and the intensity of the peak diminished, reflecting a more irregular arrangement of the clay sheets. This effect is probably due to sintering of the pillars [29] and migration of protons, which arise from the dehydration of the pillars in the clay sheets [30]. These results indicated that the Al–Ce-PILC clay sheets had not been completely destroyed even after calcination at 973 K because of the structural rigidity achieved due to pillaring. In contrast to Na-Mont, Al–Ce-PILC showed a greatly improved thermal stability.

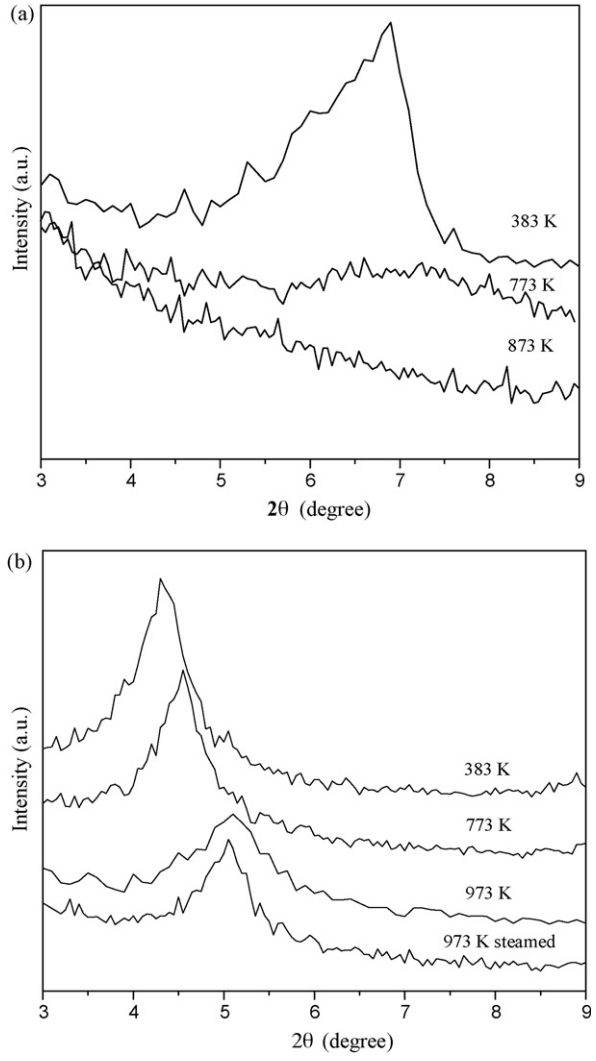

Fig. 1. XRD patterns of Na-Mont and Al–Ce-PILC. (a) Na-Mont calcined at different temperatures; (b) Al–Ce-PILC calcined at different temperatures and steamed at 973 K.

The hydrothermal stability of Al–Ce-PILC calcined at 973 K was tested by steaming the sample for 2 h at 973 K in a mixture of 20 vol% steam and 80 vol% N_2. After steaming, the intensity of the basal reflection increased, together with a decrease in the peak width, indicating a more regular pillared structure (Fig. 1b). This is in contrast with conventional Al-PILC, whose pore structure collapsed completely even at mild hydrothermal conditions. The XRD analysis demonstrated that the resulting Al–Ce-PILC had greater thermal and hydrothermal stability and can be applied as catalyst support in the SCR reaction in excess oxygen.

3.2. N_2 adsorption

The N_2 adsorption data and the corresponding basal spacing ($d_{0\,0\,1}$) values of Al–Ce-PILCs calcined at different temperatures and SO_4^{2-}/Al–Ce-PILC calcined at 773 K are given in Table 1. During pillaring, the expansion in the clay structure largely contributed to the enhancement of the surface area and porosity of the clay. The surface area analysis indicated that pillaring with Al–Ce multi-oligomeric hydroxyl cations significantly increased the surface area, from 48 m^2/g of the Na-Mont to a value around 235 m^2/g, and increased the pore volume by a factor of at least 2.4. The pore geometries of the Al–Ce-PILC samples are slit-like, without any microporosity (pores smaller than 2 nm), and the large average pore diameter in the range between 9.26 and 11.35 nm are interpreted as being caused by aggregation of clay particles into a structure like a house of cards. Although the surface area of Al–Ce-PILC declined gradually as the calcination temperature was increased, it remained as high as 168 m^2/g upon calcination at 973 K. The slight decrease in surface area at high temperatures is mainly caused by the destruction of the pore network of the clay. Compared to Al–Ce-PILC calcined at 773 K,

Table 1
N_2 adsorption data and the corresponding basal spacing $d_{0\,0\,1}$ values of Al–Ce-PILCs and SO_4^{2-}/Al–Ce-PILC

Sample	BET surface area (m^2/g)	Average pore diameter (nm)	Pore volume (m^3/g)	$d_{0\,0\,1}$ (nm)
Al–Ce-PILC (383 K)	235	9.26	0.24	2.05
Al–Ce-PILC (773 K)	227	9.30	0.24	1.94
Al–Ce-PILC (973 K)	168	11.35	0.25	1.73
SO_4^{2-}/Al–Ce-PILC (773 K)	161	12.15	0.21	1.67

both surface area and pore volume of SO_4^{2-}/Al–Ce-PILC slightly decreased to 161 m^2/g and 0.21 m^3/g, respectively. The results for N_2 adsorption revealed that the resulting Al–Ce-PILC had a high thermal stability, which agreed with the XRD results.

3.3. Effect of SO_4^{2-} modification

Fig. 2 shows how the SO_4^{2-} modification of Al–Ce-PILC enhanced the NO removal greatly. Compared with the conversions of NO and C_3H_6 on the latter catalyst (Cu/SO_4^{2-}/Al–Ce-PILC) prepared from SO_4^{2-}/Al–Ce-PILC, the NO conversion of the former catalyst (Cu/Al–Ce-PILC) supported on Al–Ce-PILC was very low, with the maximum reaching only 20% at 573 K. However, its C_3H_6 conversion was higher than that of Cu/SO_4^{2-}/Al–Ce-PILC before reaching its maximum. We conclude that the Cu/Al–Ce-PILC catalyst is active for combustion of C_3H_6 and that most of the consumed C_3H_6 is oxidized to CO_2, while SO_4^{2-} modification probably changed the acidity of the catalyst, which made the Cu/SO_4^{2-}/Al–Ce-PILC active for the partial oxidation of C_3H_6 to an active intermediate that can reduce NO, as a result, the NO conversion improved greatly, and its maximum reached 56% at 623 K.

Yang and Li reported that Brönsted acidity helped activate the hydrocarbon for the SCR of NO [31,32]. To identify the relationship between acidity and performance of the catalysts, their acidity was examined by the Py-IR method. Both catalysts evacuated at 373 K after pyridine adsorption exhibited IR bands at about 1450, 1490, 1545, 1610, and 1639 cm^{-1}. The bands at 1450 and 1610 cm^{-1} are commonly assigned to Lewis acidity, the one at 1490 cm^{-1} is mainly attributed to both Lewis and Brönsted acidity, and a small peak at 1545 cm^{-1} and the shoulder of the IR band at 1639 cm^{-1} are due to Brönsted acidity [33]. Both the Lewis and Brönsted acidity were found on the surfaces of Cu/Al–Ce-PILC and Cu/SO_4^{2-}/Al–Ce-PILC, but the bands assigned to Lewis acidity were somewhat more intense than those assigned to Brönsted acidity (Fig. 3a and b), which meant that the Lewis acidity prevailed over the Brönsted acidity. By a comparison of the catalysts, for Cu/Al–Ce-PILC, the intensities of the bands assigned to pyridine coordinated to Lewis and Brönsted acidity were reduced after increasing the evacuation temperatures. Especially, the bands at 1543 and 1639 cm^{-1} assigned to Brönsted acidity completely disappeared after evacuation at 673 K. However, for Cu/SO_4^{2-}/Al–Ce-PILC, the outstanding feature was the increase in the number and the strength of the Brönsted acidity. After the evacuation at 373 K, the bands at 1544 and 1639 cm^{-1} assigned to Brönsted acidity were much stronger than those of Cu/Al–Ce-PILC. Compared with a significant loss of intensity for Cu/Al–Ce-PILC, although the bands of Cu/SO_4^{2-}/Al–Ce-PILC also declined gradually with increasing evacuation temperature, they still existed for evacuating at 673 K.

The fact that the SO_4^{2-} modification greatly enhanced the NO conversion might be due to the increase in the number of the Brönsted acidity, to the strength of the Brönsted acidity, or to both factors. This means that Lewis acidity are active for the deep oxidization of C_3H_6 to CO_2, while Brönsted acidity promote the adsorption of C_3H_6 to form intermediates that are

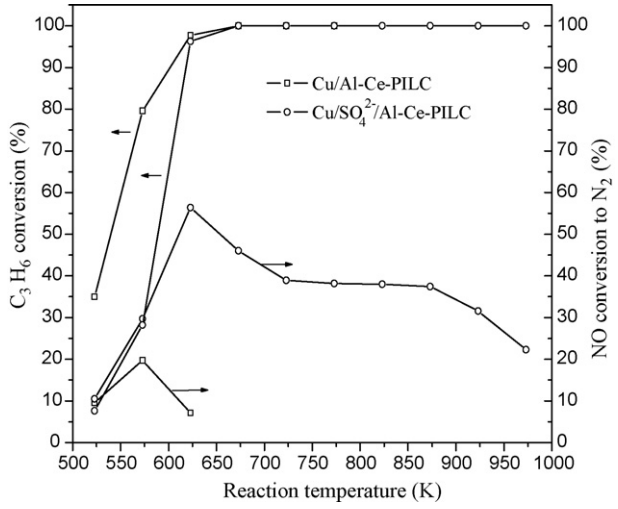

Fig. 2. Effect of SO_4^{2-} modification on the performance of the catalysts (reaction conditions: 2200 ppm NO, 1200 ppm C_3H_6, 2% O_2, helium balance, m(cat.) = 0.5 g, GHSV = 24,000 h^{-1}, 2 wt% Cu).

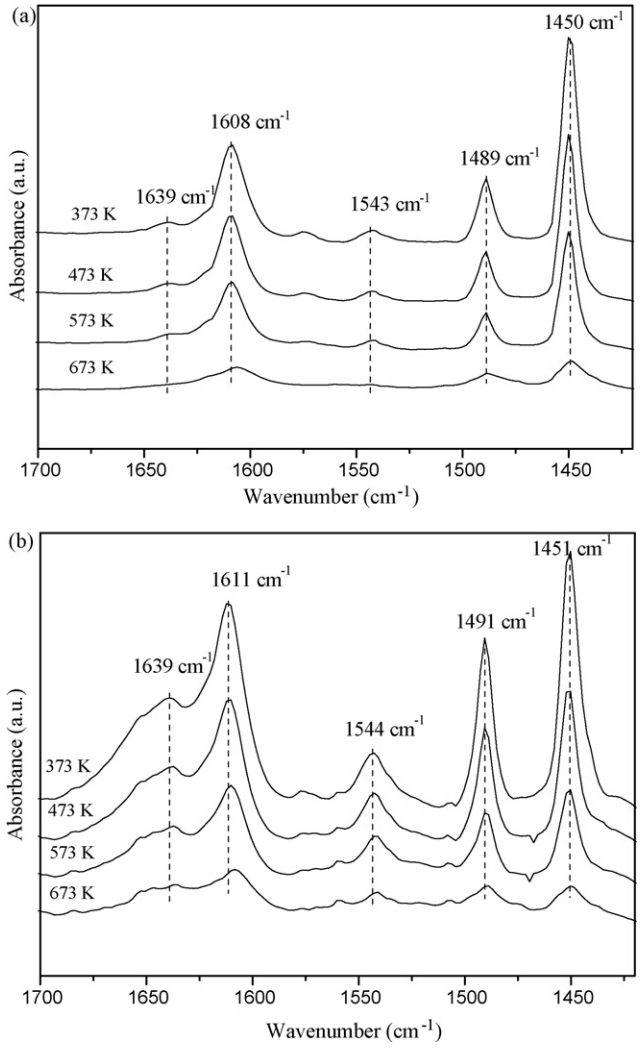

Fig. 3. IR spectra of pyridine adsorbed on the catalysts. (a) Cu/Al–Ce-PILC; (b) Cu/SO_4^{2-}/Al–Ce-PILC.

active for the reduction of NO to N_2. We conclude that Brönsted acidity are necessary for the SCR of NO by HC as Yang et al. once reported, and that the increase of Brönsted acidity plays a vital role in improving the catalytic performance. The catalysts studied in the following were all supported on SO_4^{2-}/Al–Ce-PILC.

3.4. Effect of Cu content

The NO removal was negligible at all reaction temperatures when SO_4^{2-}/Al–Ce-PILC (without copper content) was used as a catalyst for the SCR of NO, but adding copper enhanced the catalytic activity. It indicated that SO_4^{2-}/Al–Ce-PILC was inactive for the SCR of NO, while the copper species must play a significant role in this reaction [4,34]. The effect of copper content on the performance of Cu/SO_4^{2-}/Al–Ce-PILC catalysts for the SCR reaction as a function of temperature is shown in Fig. 4. Three reaction stages for NO and C_3H_6 conversion are seen. At low reaction temperatures, the NO and C_3H_6 conversion increased synchronously, as most of the consumed C_3H_6 reduced NO to N_2. With increasing temperature, C_3H_6 oxidation began to compete with NO reduction, and C_3H_6 conversion reached 100%. Although the NO conversion increased continuously and reached a maximum, the rate of increase diminished. At higher temperatures, the oxidation of C_3H_6 predominated, and NO reduction was inhibited by the depletion of the reducing agent [4].

The maximum conversion of NO increased remarkably from 42% to 56% as the Cu content increased from 1 to 2 wt% (Fig. 4a), while the corresponding temperature of maximum conversion decreased from 723 to 623 K. These two catalysts showed good performance over a broad range of temperatures, with NO conversion remaining above 22% at 973 K. However, it was observed that the NO conversion decreased and the operating range of temperature narrowed with the further increase of Cu content, the 5 wt% Cu catalyst nearly deactivated at 723 K. These results showed that the NO conversion increased with increasing Cu content until reaching an optimum of 2 wt%, while more Cu content decreased the NO conversion. On the contrary, a different behavior was observed for the conversion of C_3H_6, which the reaction temperature required for a given C_3H_6 conversion decreased with an increase of the Cu content (Fig. 4b). This may mean that different copper species exist on the catalyst surface with respect to Cu content and the NO removal depends strongly on the copper species that isolated copper ions were active for NO conversion to N_2 while CuO aggregates facilitated C_3H_6 oxidation to CO_2 [4,34,35]. Therefore, to identify the state of the copper species on the catalyst surface, TPR and XPS experiments were performed.

3.5. TPR

TPR can be used to identify and quantify metal species in catalysts. It has been reported that isolated Cu^{2+} ions can be reduced to Cu^0 by H_2 in two steps: $Cu^{2+} \rightarrow Cu^+$, $Cu^+ \rightarrow Cu^0$; while CuO is reduced directly to Cu^0 in one step, $CuO \rightarrow Cu^0$

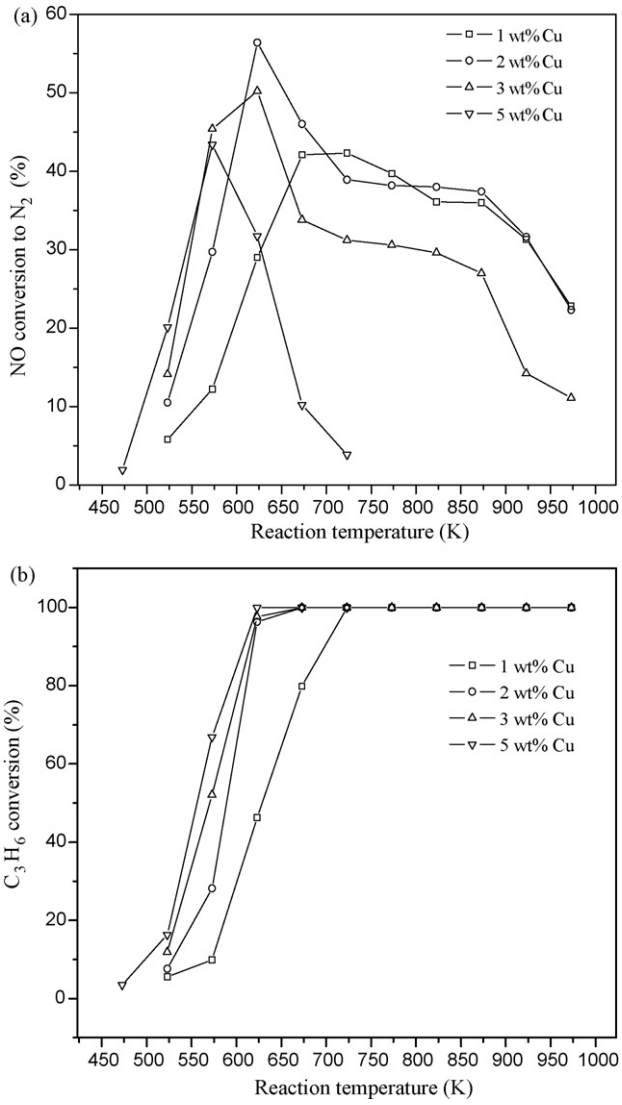

Fig. 4. Effect of Cu content on the performance of Cu/SO_4^{2-}/Al–Ce-PILC catalysts. (a) NO conversion; (b) C_3H_6 conversion (reaction conditions: 2200 ppm NO, 1200 ppm C_3H_6, 2% O_2, helium balance, m(cat.) = 0.5 g, GHSV = 24,000 h^{-1}).

[36]. No reduction peak was found with SO_4^{2-}/Al–Ce-PILC in the same range of temperature as used for the TPR measurement.

The TPR profiles of the Cu/SO_4^{2-}/Al–Ce-PILC catalysts with 2 and 5 wt% Cu are illustrated in Fig. 5. The ratio of H_2 consumption to Cu (mol/mol, measured by TPR experiment) of the catalysts with 2 wt% and 5 wt% Cu was 0.56 and 0.67, respectively, which was nearly equal to the half of Cu and main that the major copper species on the surface was Cu^+. The profile of the catalyst with 2 wt% Cu showed two reduction peaks of isolated Cu^{2+} and Cu^+ species [37,38]: the small shoulder at 733 K may be related to the process $Cu^{2+} \rightarrow Cu^+$, and the main peak at 804 K indicated that the Cu^+ existing in the catalyst and the produced Cu^+ were further reduced to Cu^0. In the catalyst with 5 wt% Cu, the peaks corresponding to the three reactions involved in the copper reduction were present as earlier mentioned. An additional reduction peak at 600 K might

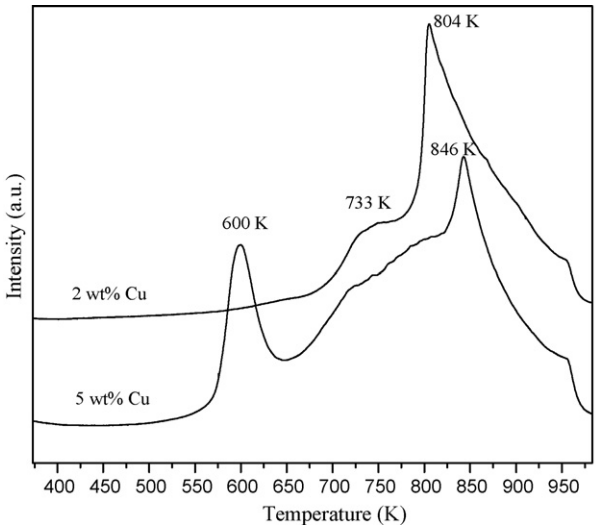

Fig. 5. TPR patterns of Cu/SO_4^{2-}/Al–Ce-PILC catalysts with different Cu contents.

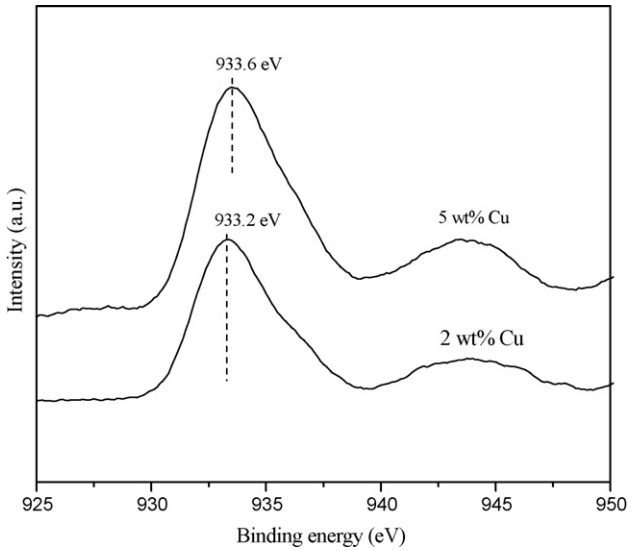

Fig. 6. Cu $2p_{3/2}$ XPS spectra of Cu/SO_4^{2-}/Al–Ce-PILC catalysts with different Cu contents.

correspond to the presence of CuO aggregates that were formed when the Cu content increased [4,26,38]. The other two reduction peaks were the same as those of the 2 wt% Cu catalyst, the peak of $Cu^{2+} \rightarrow Cu^{+}$ at medium temperature and $Cu^{+} \rightarrow Cu^{0}$ at high temperature, but smaller. The third peak was clearly shifted to higher temperature ($Cu^{+} \rightarrow Cu^{0}$), which showed that Cu^{+} species became harder to reduce as the Cu content increased. The TPR results meant that both Cu^{+} and isolated Cu^{2+} species existed in the catalyst with 2 wt% Cu, although the majority was Cu^{+}; while in the catalyst with 5 wt%, CuO aggregates were formed besides Cu^{+} and isolated Cu^{2+} species.

3.6. XPS

To further identify the copper species existing on the catalyst surface, XPS was used with the catalysts of 2 and 5 wt% copper (Fig. 6). Both catalysts showed shake-up satellite peaks at 944 eV, which were usually characteristic of Cu (II) species [39]. For the catalyst with 2 wt% Cu, the binding energy of the main Cu $2p_{3/2}$ peak was 933.2 eV. This peak could be decomposed into two parts: one caused by Cu^{+} at 932.6 eV [39], another by Cu^{2+} at a higher binding energy. For the catalyst with 5 wt% Cu, the binding energy of Cu $2p_{3/2}$ increased to 933.6 eV, which was between Cu^{+} (932.6 eV) and CuO (934.4 eV) [39]. These results showed that increasing Cu from 2 to 5 wt% increased the binding energy of Cu $2p_{3/2}$ by 0.4 eV. Since binding energy is very sensitive to chemical environment of atom, this shift indicated that a weakening of the Cu–SO_4^{2-}/Al–Ce-PILC interaction decreased the charge density of copper but increased the average oxidation state of copper in the 5 wt% Cu catalyst. The XPS results are similar to those obtained by TPR, that is, Cu^{+} and isolated Cu^{2+} species existed on the surface of the 2 wt% Cu catalyst, while another species CuO aggregates were formed as Cu content increased to 5 wt%. The higher reactivity of copper ions than CuO aggregates is the reason that the conversion of NO decreased while that of C_3H_6 increased when Cu content was increased (Fig. 4) [4,40].

3.7. Effect of water vapor

Tolerance to water is the most critical factor in developing commercial SCR catalysts. Although Cu-ZSM-5 has been the most extensively studied catalyst for the SCR of NO by HC, it suffers from severe and rapid deactivation by exposure to low concentration of water vapor [41].

The influence of water vapor in the feed on the performance of catalyst 2 wt% Cu/SO_4^{2-}/Al–Ce-PILC was studied. Fig. 7 shows the performance of this catalyst at different reaction conditions. The presence of 10% water vapor in the feed inhibited the SCR of NO causing a shift of the conversion versus temperature curve to higher temperatures, and the inhibition by water vapor was more pronounced at low

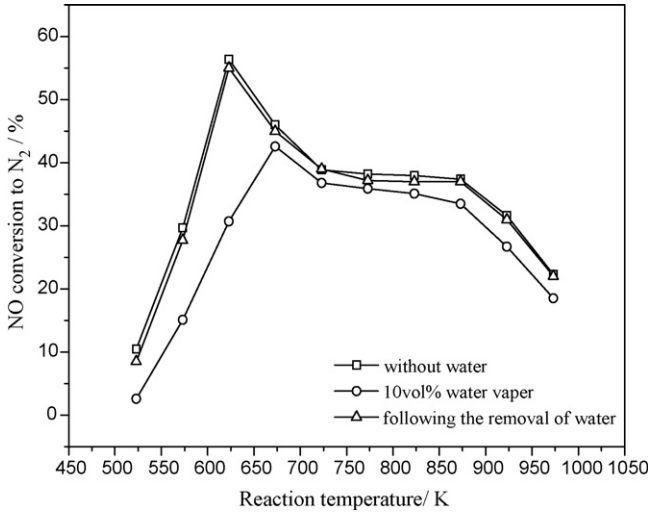

Fig. 7. Effect of steam on the performance of 2 wt% Cu/SO_4^{2-}/Al–Ce-PILC catalyst (reaction conditions: 2200 ppm NO, 1200 ppm C_3H_6, 2% O_2, 0% or 10% water vapor, helium balance, m(cat.) = 0.5 g, GHSV = 24,000 h^{-1}).

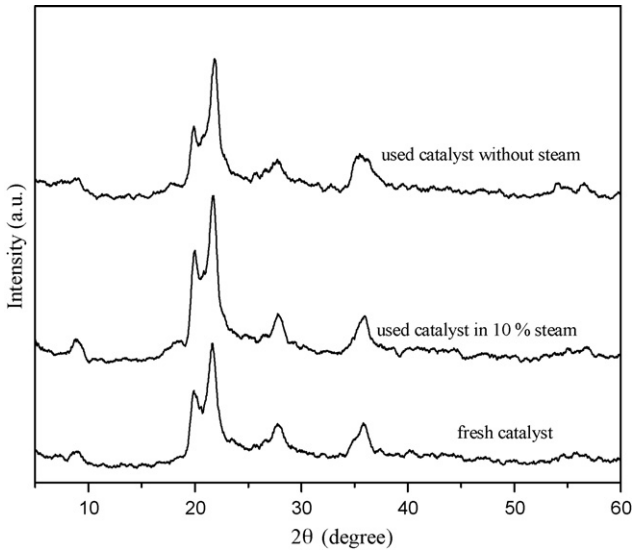

Fig. 8. XRD patterns of the fresh and used 2 wt% Cu/SO_4^{2-}/Al–Ce-PILC catalysts.

temperatures than at higher ones. However, this effect is completely reversible following the removal of water vapor from the feed. Compared to Cu-ZSM-5, the catalyst Cu/SO_4^{2-}/Al–Ce-PILC showed better resistance to water vapor, its maximum conversion of NO only decreased about 14% due to the hydrophobic nature of the oxide pillar surface [35,42]. Moreover, the XRD patterns of the catalysts (Fig. 8) also showed that 10% water vapor did not change or damage the structure of the catalyst because of its structure stability, which may be another reason for water tolerance of the catalyst. The alteration of copper ions on the surface of zeolite sintering to form inactive copper oxide clusters was known to be one of reasons for the deactivation by water [4,43,44]. However, the reversibility of the inhibition by water vapor over the catalyst Cu/SO_4^{2-}/Al–Ce-PILC suggests that chemical alteration of copper species was not expected as zeolite catalysts. The reversible loss of the activity was attributed to the competitive adsorption of water, leading to decrease adsorption property of reactants as well as the oxidative activity.

4. Conclusions

Na-Mont was pillared by multi-oligomeric hydroxyl cations to synthesize Al–Ce-PILC, which showed good thermal and hydrothermal stability. Al–Ce-PILC calcined at 773 K had a BET surface area of 227 m^2/g and an average pore diameter of 9.30 nm. It maintained a surface area as high as 168 m^2/g and a pore diameter of 11.35 nm after calcination at 973 K. Steaming gave Al–Ce-PILC a more regular pillared structure. After SO_4^{2-} modification, both surface area and pore volume of SO_4^{2-}/Al–Ce-PILC slightly decreased to 161 m^2/g and 0.21 m^3/g, respectively. The results indicated that the obtained Al–Ce-PILC could be applied to the SCR reaction as catalyst support in excess oxygen.

Both Lewis and Brönsted acidity existed on the catalysts, mainly Lewis acidity. SO_4^{2-} modification increased the number and strength of the Brönsted acidity on the surface of the Cu/SO_4^{2-}/Al–Ce-PILC catalyst, which played a vital role in the great improvement in the performance of the catalyst prepared by impregnation. The 2 wt% Cu catalyst showed good performance over a broad range of temperature; its maximum conversion of NO to N_2 was 56% at 623 K and 22% at 973 K, with a feed of 2200 ppm NO, 1200 ppm C_3H_6, 2% O_2, and helium as balance at a space velocity of 24,000 h^{-1}. The catalytic performance greatly depended on the copper species. TPR and XPS showed that both Cu^+ and isolated Cu^{2+} species existed in the optimal catalyst, the majority was Cu^+. When the Cu content was increased to 5 wt%, besides Cu^+ and isolated Cu^{2+}, another species CuO aggregates which facilitated the combustion of C_3H_6 and inhibited the reduction of NO were formed. Finally, the presence of 10% water vapor in the feed only slightly decreased its catalytic performance due to the hydrophobic nature of the oxide pillar surface and the structural stability of the Cu/SO_4^{2-}/Al–Ce-PILC. However, this effect was reversible following the removal of water from the gas stream, which was attributed to the competitive adsorption of water and the reactants on the active sites.

Acknowledgements

This work was financially supported by grants from the Key Programs of the National Natural Science Foundation of China (No. 20437010) and the Chinese Postdoctoral Science Foundation (No. 2005037058). The authors are grateful to Professor Roel Prins and Professor Kenneth A. Rahn for providing helpful advice to improve our paper.

References

[1] 93/59/EC European Community Legislation.
[2] 96/69/EC European Community Legislation.
[3] 98/69/EC European Community Legislation.
[4] R.T. Yang, N. Tharappiwattananon, R.Q. Long, Appl. Catal. B 19 (1998) 289.
[5] J. Wang, H. He, Q.C. Feng, Y.B. Yu, K. Yoshida, Catal. Today 93–95 (2004) 783.
[6] L. Gutierrez, E.A. Lombardo, J.O. Petunchi, Appl. Catal. A 194/195 (2000) 169.
[7] H. Ohtsuka, T. Tabata, Appl. Catal. B 29 (2001) 177.
[8] E. Seker, N. Yasyerli, E. Gulari, C. Lambert, R.H. Hammerle, Appl. Catal. B 37 (2002) 27.
[9] A.A. Nikolopoulos, E.S. Stergioula, E.A. Efthimiadis, I.A. Vasalos, Catal. Today 54 (1999) 439.
[10] R. Burch, D. Ottery, Appl. Catal. B 13 (1997) 105.
[11] H. He, J. Wang, Q.C. Feng, Y.B. Yu, K. Yoshida, Appl. Catal. B 46 (2003) 365.
[12] J.H. Li, J.M. Hao, L.X. Fu, Z.M. Liu, X.Y. Cui, Catal. Today 90 (2004) 215.
[13] K.I. Shimizu, A. Satsuma, T. Hattori, Catal. Surv. Jpn. 4 (2000) 115.
[14] H. He, C.B. Zhang, Y.B. Yu, Catal. Today 90 (2004) 191.
[15] M.C. Kung, P.W. Park, D.-W. Kim, H.H. Kung, J. Catal. 181 (1999) 1.
[16] P.W. Park, H.H. Kung, D.-W. Kim, M.C. Kung, J. Catal. 184 (1999) 440.
[17] A. Ueda, T. Oshima, M. Haruta, Appl. Catal. B 12 (1997) 81.
[18] T. Maunula, Y. Kintaichi, M. Haneda, H. Hamada, Catal. Lett. 61 (1999) 121.
[19] S. Matsumoto, Catal. Today 29 (1996) 43.
[20] Y. Wan, J.X. Ma, Z. Wang, W. Zhou, S. Kaliaguine, J. Catal. 227 (2004) 242.
[21] I.M. Saaid, A.R. Mohamed, S. Bhatia, J. Mol. Catal. A 189 (2002) 241.

[22] Q.C. Lin, W.M. Lin, J.M. Hao, J.H. Li, L.X. Fu, Chem. J. Chin. Univ. 27 (2006) 85.
[23] M. Ogura, M. Hayashi, E. Kikuchi, Catal. Today 45 (1998) 139.
[24] A. Gil, L.M. Gandia, M.A. Vicente, Catal. Rev-Sci. Eng. 42 (2000) 145.
[25] Z. Ding, J.T. Kloprogge, R.L. Frost, J. Porous Mater. 8 (2001) 273.
[26] J.L. Valverde, A. de Lucas, P. Sánchez, F. Dorado, A. Romero, Appl. Catal. B 43 (2003) 43.
[27] W.B. Li, M. Sirilumpen, R.T. Yang, Appl. Catal. B 11 (1997) 347.
[28] G.R. Rao, B.G. Mishra, React. Kinet. Catal. Lett. 75 (2002) 251.
[29] F. Figueras, A. Mattrod-Bashi, G. Fetter, A. Thrierr, J.V. Zanchetta, J. Catal. 119 (1989) 91.
[30] H.Y. Zhu, N. Maes, A. Molinard, E.F. Vansant, Micropor. Mater. 3 (1994) 235.
[31] R.T. Yang, W.B. Li, J. Catal. 155 (1995) 414.
[32] M. Shelef, Chem. Rev. 95 (1995) 209.
[33] Y.G. Yin, Research Methods of Heterogeneous Catalysts, Chemical Industry Press, Beijing, 1988, p. 582.
[34] M. Sirilumpen, R.T. Yang, N. Tharapiwattananon, J. Mol. Catal. A 137 (1999) 273.
[35] B.S. Kim, S.H. Lee, Y.T. Park, S.W. Ham, H.J. Chae, I.S. Nam, Korean J. Chem. Eng. 18 (2001) 704.
[36] G. Delahay, B. Coq, L. Broussous, Appl. Catal. B 12 (1997) 49.
[37] S. Tanabe, H. Matsumoto, Appl. Catal. 45 (1988) 27.
[38] R. Bulánek, B. Wichterlová, Z. Sobalíc, J. Tichý, Appl. Catal. B 31 (2001) 13.
[39] J.Q. Wang, W.H. Wu, D.M. Feng, Introduction to Electron Energy Spectrum, National Defense Industry Press, Beijing, July 8–10, 1992 , p. 77.
[40] J.Y. Yan, W.M.H. Sachtler, H.H. Kung, Catal. Today 33 (1997) 279.
[41] J.N. Armor, Appl. Catal. B 4 (1994) N18.
[42] Y.S. Han, S. Yamanaka, J.H. Choy, J. Solid State Chem. 144 (1999) 45.
[43] F.C. Meunier, R. Ukropec, C. Stapleton, J.R.H. Ross, Appl. Catal. B 30 (2000) 163.
[44] Z. Chajar, P. Denton, F.B. de Bernard, M. Primet, H. Praliaud, Catal. Lett. 55 (1998) 217.